

Showcasing a *Perspective* from Dr. Sayaka Uchida, School of Arts and Sciences, The University of Tokyo, Japan

Frontiers and progress in cation-uptake and exchange chemistry of polyoxometalate-based compounds

Cation-uptake and exchange in polyoxometalates (POMs) and POM-based compounds are categorized and reviewed in three groups: POMs as inorganic crown ethers and cryptands, POM-based ionic solids as cation-exchangers, and reduction-induced cation-uptake in POM-based ionic solids, which is based on a feature of POMs that they are redox-active and multi-electron transfer occurs reversibly in multiple-steps. This method can be utilized to synthesize mixed-valence metal clusters in metal ion-exchanged POM-based ionic solids.

As featured in:



See Sayaka Uchida, *Chem. Sci.*, 2019, **10**, 7670.



Cite this: *Chem. Sci.*, 2019, **10**, 7670

All publication charges for this article have been paid for by the Royal Society of Chemistry

Received 10th June 2019  
Accepted 24th July 2019

DOI: 10.1039/c9sc02823d  
[rsc.li/chemical-science](http://rsc.li/chemical-science)

## Frontiers and progress in cation-uptake and exchange chemistry of polyoxometalate-based compounds

Sayaka Uchida 

Cation-uptake and exchange has been an important topic in both basic and applied chemistry relevant to life and materials science. For example, living cells contain appreciable amounts of  $\text{Na}^+$  and  $\text{K}^+$ , and their concentrations are regulated by the sodium–potassium pump. Solid-state cation-exchangers such as clays and zeolites both natural and synthetic have been used widely in water softening and purification, separation of metal ions and biomolecules, etc. Polyoxometalates (POMs) are robust, discrete, and structurally well-defined metal-oxide cluster anions, and have stimulated research in broad fields of sciences. In this perspective, cation-uptake and exchange in POM and POM-based compounds are categorized and reviewed in three groups: (i) POMs as inorganic crown ethers and cryptands, (ii) POM-based ionic solids as cation-exchangers, and (iii) reduction-induced cation-uptake in POM-based ionic solids, which is based on a feature of POMs that they are redox-active and multi-electron transfer occurs reversibly in multiple steps. This method can be utilized to synthesize mixed-valence metal clusters in metal ion-exchanged POM-based ionic solids.

### 1. Introduction

Cation-uptake and exchange from aqueous solutions has been an important topic in both basic and applied chemistry relevant to life and materials science.<sup>1–3</sup> For example, living cells contain appreciable amounts of  $\text{Na}^+$  and  $\text{K}^+$ , and their concentrations

are regulated by the sodium–potassium pump, which exchanges three  $\text{Na}^+$  with two  $\text{K}^+$ .<sup>3</sup> On the other hand, it is quite difficult to achieve high selectivity towards  $\text{K}^+$  artificially except for 18-crown-6 ether,<sup>4</sup> which is a cyclic oligomer of ethylene oxide, and binds  $\text{K}^+$  by using all six oxygens as donor atoms. The denticity of the polyether influences the affinity toward various ions: 15-crown-5 and 12-crown-4 show high selectivity toward  $\text{Na}^+$  and  $\text{Li}^+$ , respectively. Crown ethers have been widely used for cation recognition and separation, and as phase transfer catalysts.<sup>5</sup>

Solid-state cation-exchangers play an especially important role in chemistry. A classic example is zeolites, which are microporous crystalline aluminosilicates with anionic frameworks due to the substitution of  $\text{Si}^{4+}$  by  $\text{Al}^{3+}$ .<sup>6</sup> Cations such as  $\text{Na}^+$ ,  $\text{K}^+$ ,  $\text{Ca}^{2+}$ ,  $\text{Mg}^{2+}$ , etc. loosely interact with the anionic framework via Coulomb interaction, which can be exchanged by treating the zeolite in an aqueous solution containing excess amount of foreign cations. It is well known that the pore sizes and adsorption properties of zeolites can be controlled by the types of cations: the effective pore size of Linde Type A (LTA) zeolite with  $\text{K}^+$  is 3 Å (Molecular Sieves 3A), and the pore size is increased to 4 Å by the exchange of  $\text{K}^+$  with smaller  $\text{Na}^+$  (Molecular Sieves 4A).<sup>7</sup> Zeolites can adsorb gas and vapor ( $\text{CH}_4$ ,  $\text{H}_2\text{O}$ , etc.) in the microporous structure, and the amounts of adsorption in alkaline earth metal ion-exchanged and alkali metal ion-exchanged faujasite (FAU) zeolites increase with the increase in the ionic potentials  $z/r$  ( $z$  and  $r$  are the charge and radius of the ion, respectively) of the counter cations.<sup>8,9</sup>



Sayaka Uchida is an associate professor at the Department of Basic Science, The University of Tokyo (Japan). She received her PhD in applied chemistry from The University of Tokyo (2002). She has worked as a postdoc and assistant professor at the Department of Applied Chemistry, The University of Tokyo (Prof. Noritaka Mizuno group) and moved to the current position (2009 Oct). She has also worked

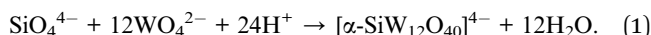
as a JST-PRESTO researcher “Hyper-nanospace design toward innovative functionality” (2013–2017). Her work focuses on the synthesis of functional solid-state materials based on polyoxometalates.



Recently, because of relatively facile reaction conditions, cation-exchange has also been recognized as a strategy for post-synthesis and discovery of new solid materials.<sup>2</sup> Metal-organic frameworks (MOFs), which can be recognized as “inorganic-organic zeolites” have emerged decades ago, but cation-exchange has been reported only recently. A landmark report in this research area is the exchange of guest  $Mn^{2+}$  in as-synthesized  $Mn_3[(Mn_4Cl_3)(BTT)_8(CH_3OH)_{10}]_2$  (BTT = 1,3,5-benzenetriacetate) with monovalent or divalent metal ions in methanol solution, which resulted in the formation of iso-structural frameworks with a large variation in  $H_2$  adsorption enthalpy.<sup>10,11</sup> Cation-exchange has been also employed with nanocrystals and nanoparticles to fine-tune their structures and functions systematically.<sup>12</sup> For example, *in vivo* cation-exchange

of  $Ag^+$  with  $Hg^{2+}$  and  $Zn^{2+}$  in selenide/sulfide quantum dots enhanced the specificity of tumor imaging.<sup>13</sup>

Polyoxometalates (POMs) are robust, discrete, and structurally well-defined oxide cluster anions that are mainly composed of high-valence transition metals (such as  $W^{6+}$ ,  $Mo^{6+}$ ,  $V^{5+}$ ) and have stimulated research in broad fields of sciences.<sup>14–25</sup> For example,  $\alpha$ -Keggin-type silicododecatungstate, which is one of the most researched and popular POM, forms according to the following equation:



The oxides of high-valence transition metals dissolve at high pH as an anion (e.g.,  $WO_4^{2-}$ ), condensation proceeds *via* loss of

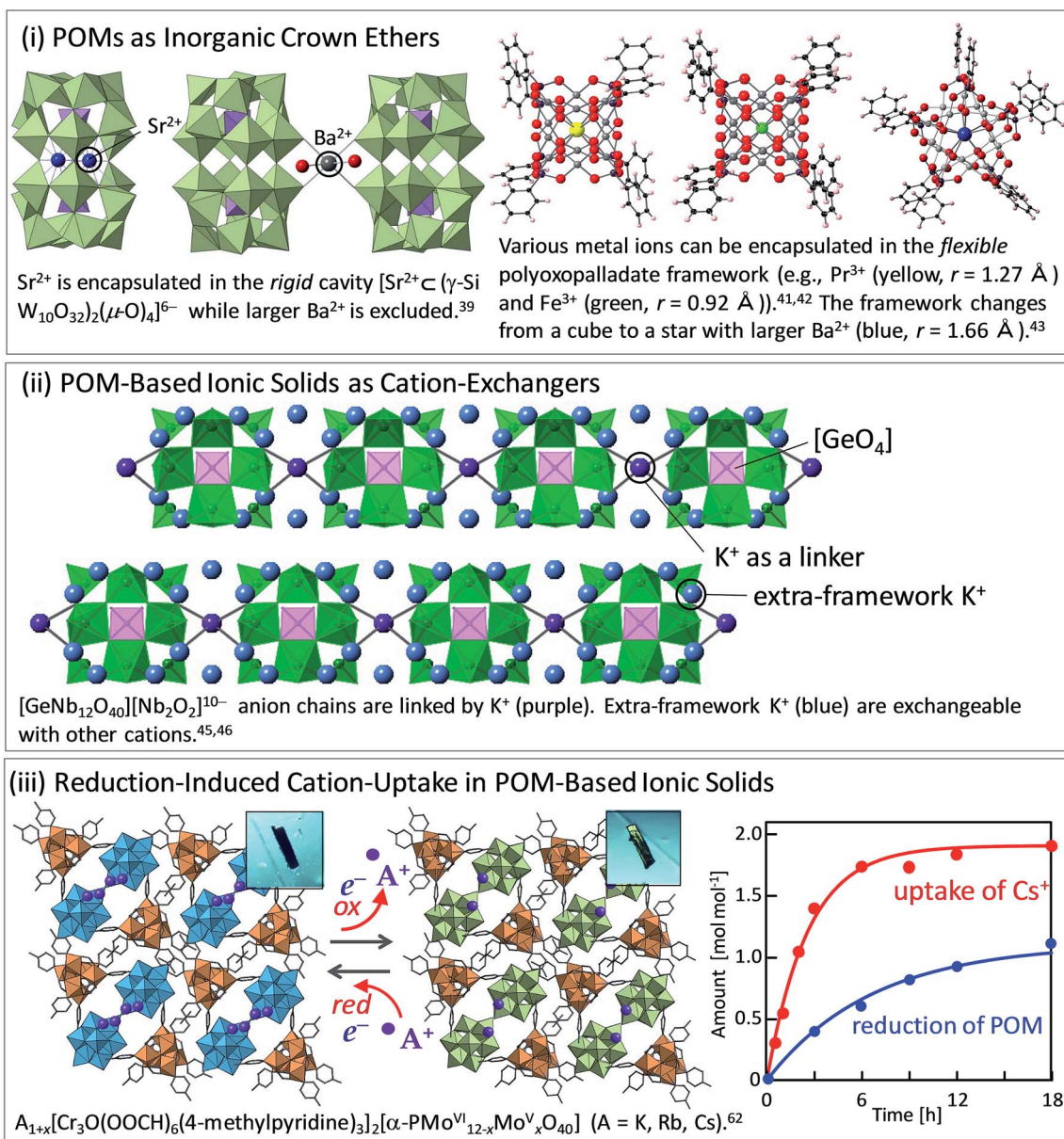
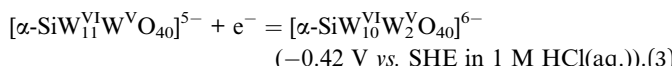
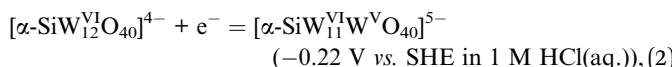


Fig. 1 Cation-uptake and exchange in POM and POM-based compounds categorized in three groups: (i) POMs as inorganic crown ethers, (ii) POM-based ionic solids as cation-exchangers, and (iii) reduction-induced cation-uptake in POM-based ionic solids.



water and formation of M–O–M linkages with acidification, and an anionic molecular framework of twelve octahedral tungsten oxoanions surrounding a central silicate is formed. One of the most noteworthy features of POMs are that they are redox-active, and multi-electron transfer occurs reversibly in multiple-steps.<sup>16</sup>



In this perspective, cation-uptake and exchange in POM and POM-based compounds are categorized and reviewed in three groups: (i) POMs as inorganic crown ethers and cryptands, (ii) POM-based ionic solids as cation-exchangers, and (iii) reduction-induced cation-uptake in POM-based ionic solids (Fig. 1). Unique functions related to these cation-exchanged POM-based compounds are introduced, and future works arising from these functions are also discussed. For past developments on polyoxometalates as cation-exchangers, the readers are directed to a legendary review article.<sup>26</sup>

## 2. Polyoxometalates as inorganic crown ethers and cryptands

Crown ethers<sup>4,5</sup> and cryptands,<sup>27,28</sup> which are a family of synthetic cyclic and polycyclic multidentate organic ligands, have attracted great interest due to their structural topologies and applications especially in selective cation-uptake. Crown ethers can strongly bind alkali and alkali earth metal ions size-selectively with the oxygen donors in gas, solution, or solid phases. Cryptands can bind these cations using both nitrogen and oxygen donors three-dimensionally, often showing higher selectivity and binding constants.

In contrast, POMs can serve as inorganic crown ethers and cryptands:<sup>29</sup> an early example is a cyclic POM  $[\text{As}_4\text{W}_{40}\text{O}_{140}]^{28-}$ , which binds alkali and alkaline earth metal ions selectively within the central “cryptand site” (best fit for  $\text{K}^+$  and  $\text{Ba}^{2+}$ , which are hard Lewis acids) while transition metals (soft Lewis acids) bind to the “external site” with a different type of coordination.<sup>30</sup> A recent work by Kortz and co-workers on a wheel-shaped  $\text{K}^+$ -templated POM  $[\text{K} \subset \{(\beta\text{-As}^{\text{III}}\text{W}_8\text{O}_{30})(\text{WO}(\text{H}_2\text{O}))\}_3]^{14-}$  exhibits high selectivity to  $\text{Rb}^+$ , because the size of the central cavity is relatively large for  $\text{K}^+$ .<sup>31</sup> Preyssler–Pope–Jeannin-type POM with a general formula of  $[\text{X}^{n+}(\text{H}_2\text{O})\text{P}_5\text{W}_{30}\text{O}_{110}]^{(15-n)-}$  is the smallest POM with an internal cavity allowing cation-exchange in aqueous solutions.<sup>32,33</sup> Preyssler–Pope–Jeannin-type POM possesses a flexible  $\text{W}_5\text{O}_5$  cavity and can capture various cations from  $\text{Na}^+$ ,  $\text{Ca}^{2+}$ ,  $\text{La}^{3+}$  to tetravalent actinides (e.g.,  $\text{Th}^{4+}$ ) (Fig. 2),<sup>34</sup> so that they have been considered as a potentially useful material for separation of nuclear wastes. DFT calculations by López, Poblet, and co-workers have revealed that encapsulation of cations with larger charge is difficult (*i.e.*, heating is needed) because energy cost for the cation encapsulation from aqueous solution is dependent on the dehydration enthalpy of the

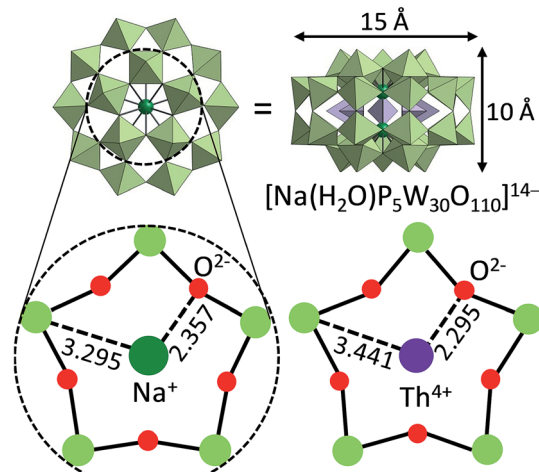


Fig. 2 Preyssler–Pope–Jeannin-type POM  $[\text{X}^{n+}(\text{H}_2\text{O})\text{P}_5\text{W}_{30}\text{O}_{110}]^{(15-n)-}$  with flexible  $\text{W}_5\text{O}_5$  cavity for cation encapsulation.<sup>33</sup> Light green and purple polyhedra show the  $[\text{WO}_6]$  and  $[\text{PO}_4]$  units, respectively.

cation.<sup>34</sup> A more recent report by Li, Su, Wang and co-workers shows that while Preyssler–Pope–Jeannin-type POMs with phosphorous  $[\text{P}_5\text{W}_{30}\text{O}_{110}]^{15-}$  exhibit high affinity to  $\text{Na}^+$ , those with sulfur  $[\text{S}_5\text{W}_{30}\text{O}_{110}]^{10-}$  exhibit high affinity to  $\text{K}^+$  because of the larger internal cavity.<sup>35</sup>

Müller and co-workers synthesized a series of nanoporous POM capsules with a general formula of  $[(\text{Mo}^{\text{VI}})\text{Mo}^{\text{VI}}_5\text{O}_{21}(\text{H}_2\text{O})_6]_{12}[\text{Mo}^{\text{V}}_2\text{O}_4(\text{ligand})]_{30}$ , and these capsules allow systematic studies of uptake/release of cations in aqueous solutions.<sup>36,37</sup> The capsules possess large negative charges, and the affinity and coordination environment for cations depend on the functional groups inside the capsules. For example, various cations can coordinate to  $\text{SO}_4^{2-}$  ligands *via* exchange with  $\text{NH}_4^+$ : protonated urea molecules situate close to the pore openings while  $\text{Ce}^{3+}$  situates deeply inside the capsule due to the small ionic radius (Fig. 3).<sup>36,37</sup> The protonated urea molecules can be removed and the pores open by cation-exchange with  $\text{Ca}^{2+}$  in water.<sup>38</sup> This system can be recognized as an artificial cell since  $\text{Ca}^{2+}$  take an important role in life science.

Mizuno and co-workers synthesized a dimeric POM  $[\text{H}_n(\gamma\text{-SiW}_{10}\text{O}_{32})_2(\mu\text{-O})_4]^{(8-n)-}$  by dehydrative condensation of

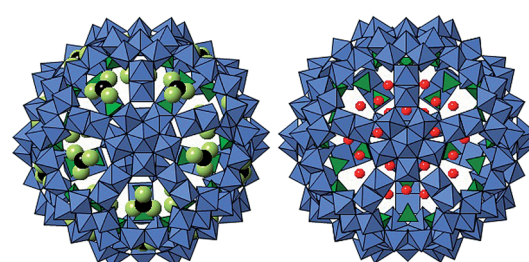


Fig. 3 Coordination environments of protonated urea (left, black: C and yellow: N/O) and  $\text{Ce}^{3+}$  (right, red) in the nanoporous POM capsule.<sup>36,37</sup> Blue and green polyhedra show the  $[\text{MO}_6]$  and  $[\text{SO}_4]$  units, respectively.

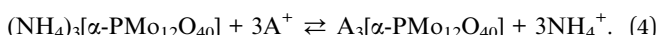


silicodectungstate  $[\gamma\text{-SiW}_{10}\text{O}_{34}(\text{H}_2\text{O})_2]^{4-}$ .<sup>39</sup> The dimeric POM has a rigid cavity between the two silicodectungstate units, where divalent  $\text{Pb}^{2+}$  and  $\text{Sr}^{2+}$  and monovalent  $\text{Ag}^+$ ,  $\text{Na}^+$ ,  $\text{K}^+$ , and  $\text{Rb}^+$  can be encapsulated, while larger  $\text{Ba}^{2+}$  and  $\text{Cs}^+$  are completely excluded (Fig. 1). Interestingly, this POM, which can be considered as an inorganic cryptand, can capture  $\text{Sr}^{2+}$  more strongly than the organic counterpart. Baskar, Winpenny, and co-workers have reported that a  $\epsilon$ -Keggin-type POM constructed with  $[\text{SbO}_6]$  units can accommodate  $d^5$  and  $d^{10}$  ions such as  $\text{Mn}^{2+}$  and  $\text{Zn}^{2+}$  at the center cage of the molecule in a tetrahedral fashion.<sup>40</sup>

Kortz and co-workers have reported that a polyoxopalladate  $[\text{MPd}_{12}^{II}(\text{AsPh})_8\text{O}_{32}]^{n-}$  can accommodate various lanthanide ions ( $\text{M} = \text{Pr}^{3+}$ ,  $\text{Nd}^{3+}$ ,  $\text{Sm}^{3+}$ ,  $\text{Eu}^{3+}$ ,  $\text{Gd}^{3+}$ ,  $\text{Tb}^{3+}$ ,  $\text{Dy}^{3+}$ ,  $\text{Ho}^{3+}$ ,  $\text{Er}^{3+}$ ,  $\text{Tm}^{3+}$ ,  $\text{Yb}^{3+}$ ,  $\text{Lu}^{3+}$ ) as well as 3d transition metal ions ( $\text{M} = \text{Sc}^{3+}$ ,  $\text{Mn}^{2+}$ ,  $\text{Fe}^{3+}$ ,  $\text{Co}^{2+}$ ,  $\text{Cu}^{2+}$ ,  $\text{Zn}^{2+}$ ) at the cuboidal center cage of the molecule.<sup>41,42</sup> The  $[\text{Pd}_{12}\text{O}_{32}]$  unit is flexible and can adjust to the coordination requirements of a large variety of metal ions (Fig. 1).<sup>41,42</sup> More recently, they have reported that alkaline earth metal ions ( $\text{Ca}^{2+}$ ,  $\text{Sr}^{2+}$ ,  $\text{Ba}^{2+}$ ) with relatively large ionic radii as templates affect the polyoxopalladate framework so that the nanocube (8-coordination) transforms to a nanostar (10-coordination).<sup>43</sup>

### 3. Polyoxometalate-based ionic solids as cation-exchangers

Ammonium salt of  $\alpha$ -Keggin-type phosphododecamolybdate  $(\text{NH}_4)_3[\alpha\text{-PMo}_{12}\text{O}_{40}]$  has been long investigated as a cation-exchanger in aqueous solutions according to the following equation,



The following affinity was derived  $\text{Cs}^+ > \text{Tl}^+ > \text{Rb}^+ > \text{Ag}^+ > \text{K}^+ > \text{H}_3\text{O}^+ > \text{Na}^+ > \text{Li}^+$ , which is in line with the trend in hydration radius or dehydration enthalpy of the cations.<sup>26,44</sup> This trend means that it is more facile to remove the water of hydration from  $\text{Cs}^+$  than  $\text{Li}^+$  because of the large ionic radius (*i.e.*, low ionic potential) of  $\text{Cs}^+$ , so that  $\text{Cs}^+$  can more easily enter and diffuse through the solid state structure. Besides,  $[\alpha\text{-PMo}_{12}\text{O}_{40}]^{3-}$  shows high affinity towards  $\text{Tl}^+$  or  $\text{Ag}^+$ , and the bonds between  $\text{Tl}^+$  or  $\text{Ag}^+$  and  $\text{O}^{2-}$  of the POM are supposed to have a covalent character.

The selectivity, kinetics, and capacity of cation-exchange in POM-based ionic solids are determined both by the framework geometry and the behavior of extra-framework cations. For example, Nyman and co-workers reported that Keggin-type polyoxoniobates  $[\text{XNb}_{12}\text{O}_{40}]^{n-}$  ( $\text{X} = \text{Si, Ge, P}$ ) with  $[\text{Ti}_2\text{O}_2]^{4+}$  or  $[\text{Nb}_2\text{O}_2]^{4+}$  bridges form one-dimensional chains, and these chains have an overall negative charge of  $-10$  or  $-12$ .<sup>45</sup> Single crystal X-ray diffraction, thermogravimetry, IR, and  $^{1}\text{H}$ -MASNMR combined with computational studies could distinguish the states of counter cations ( $\text{Na}^+$  and  $\text{K}^+$ ), and the mobile extra-framework cations can be exchanged with radionuclides ( $\text{Sr}^{2+}$ ,  $\text{Np}(\text{NpO}_2^+)$ , and  $\text{Pu}^{4+}$ ) (Fig. 1).<sup>46</sup> Unlike with conventional POMs, polyoxoniobates are stable under basic conditions, and therefore should be less likely to decompose in the highly alkaline

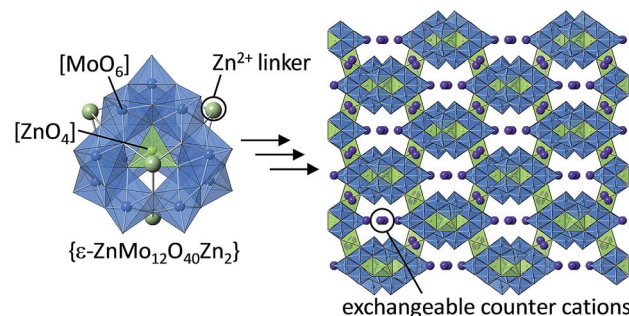


Fig. 4 Microporous solid composed of  $\{\epsilon\text{-ZnMo}_{12}\text{O}_{40}\text{Zn}_2\}$  units and exchangeable counter cations.<sup>47</sup>

conditions of nuclear wastes. More recently, Ueda, Sadakane, and co-workers synthesized microporous solids with  $\epsilon$ -Keggin-type POMs and  $\text{Zn}^{2+}$  or  $\text{Mn}^{2+}$  as linkers (Fig. 4).<sup>47</sup> These solids possess 3D-cages and channels with an aperture of *ca.* 8 Å containing exchangeable cations ( $\text{NH}_4^+$  and  $\text{Na}^+$ ). These cations can be exchanged with  $\text{K}^+$ ,  $\text{Rb}^+$ , and  $\text{Cs}^+$  in aqueous solutions, while exchange with  $\text{H}^+$  and  $\text{Li}^+$  is insufficient,<sup>47</sup> which is in line with the hydration radius and dehydration enthalpy of the cations.<sup>44</sup> More recently, the same group has reported the synthesis and structure of a polyoxomolybdate with a one-dimensional molecular structure.<sup>48</sup>  $\text{NH}_4^+$  as counter cations surround the molecular wire, and  $\text{NH}_4^+$  is selectively exchanged with  $\text{Cs}^+$  among alkali metal ions in water, and large alkylammonium cations can also be incorporated due to the flexible solid-state structure.<sup>49</sup>

Acidic salts of  $\alpha$ -Keggin-type POM ( $\text{H}_3[\alpha\text{-PW}_{12}\text{O}_{40}]\cdot n\text{H}_2\text{O}$ ,  $\text{H}_4[\alpha\text{-SiW}_{12}\text{O}_{40}]\cdot n\text{H}_2\text{O}$ ) have been well known as excellent acid catalysts, and partial substitution of protons with  $\text{Cs}^+$  in aqueous solutions, stabilizes the solid-state structure and increases the surface area.<sup>50-52</sup> The cesium hydrogen salt of silicodectungstate  $\text{Cs}_x\text{H}_{4-x}[\alpha\text{-SiW}_{12}\text{O}_{40}]$  adopts a body-centered cubic cell in analogy to the cesium salt of phosphododecamolybdate  $\text{Cs}_3[\alpha\text{-PW}_{12}\text{O}_{40}]$ .<sup>53</sup> We have shown that the use of  $[\alpha\text{-SiW}_{12}\text{O}_{40}]^{4-}$  instead of  $[\alpha\text{-PW}_{12}\text{O}_{40}]^{3-}$  leads to the formation of POM vacancies to compensate the excess negative charge, which give rise to channels exhibiting cation-exchange of  $\text{Cs}^+$  with other alkali metal ions in aqueous solutions (Fig. 5a and b).<sup>54</sup> Amounts of cation-exchange decreased in the order of  $\text{Rb}^+ > \text{K}^+ > \text{Na}^+ > \text{Li}^+$ , which is in line with the hydration radius and dehydration enthalpy of the alkali metal ions<sup>44</sup> (Fig. 5c), and elemental mapping images confirmed the uniform distribution of the exchanged cations (Fig. 5d).<sup>54</sup> Recently, Sun and co-workers showed that the cation-exchange of  $\text{Cs}^+$  in the cesium hydrogen salt of silicodectungstate with Bi ( $\text{BiO}^+$  and  $\text{BiOH}^{2+}$ ) having stereoactive  $6s^2$  lone pair as a dopant, leads to near-infrared photoluminescence in the important biological and telecommunication optical windows, due to the asymmetric coordination geometry of the Bi species in the microporous framework.<sup>55</sup> This result offers a new strategy for the preparation of POM-based luminescent systems *via* cation-exchange.

We have reported a porous organic-inorganic ionic crystal  $\text{K}_2[\text{Cr}_3\text{O}(\text{OOC})_6(4\text{-methylpyridine})_3]_2[\alpha\text{-SiW}_{12}\text{O}_{40}]\cdot n\text{H}_2\text{O}$  composed of  $[\alpha\text{-SiW}_{12}\text{O}_{40}]^{4-}$  with a molecular cation



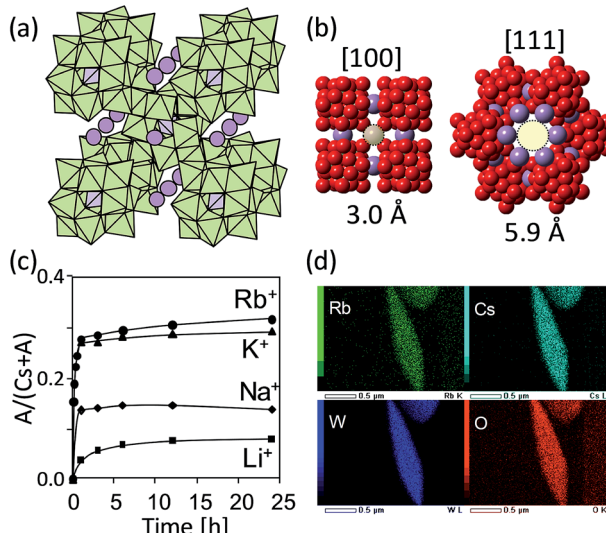


Fig. 5 (a) Crystal structure of  $\text{Cs}_x\text{H}_{4-x}[\alpha\text{-SiW}_{12}\text{O}_{40}]$ . Light green and orange polyhedra show the  $[\text{WO}_6]$  and  $[\text{SiO}_4]$  units, respectively. Purple spheres are exchangeable cations ( $\text{Cs}^+$ ). (b) Anion vacancies (in light yellow) along the [100] and [111] directions. Red and purple spheres show the  $\text{O}^{2-}$  of POM and  $\text{Cs}^+$ , respectively. (c) Cation-exchange: time courses of uptakes of alkali metal ions. (d) Elemental mapping images.<sup>54</sup>

$[\text{Cr}_3\text{O}(\text{OOCH})_6(4\text{-methylpyridine})_3]^+$ , which possess robust one-dimensional channels due to  $\pi$ - $\pi$  stacking among the 4-methylpyridine of the neighboring cations.<sup>56</sup>  $\text{Cr}^{(\text{III})}$ -carboxylates with a general formula of  $[\text{Cr}_3\text{O}(\text{OOCR})_6(\text{L})_3]^+$  have been widely considered as building blocks of porous solids because of the versatile selection of bridging (R) and terminal (L) ligands and chemical inertness due to the large crystal field stabilization energy of  $\text{Cr}^{3+}$  with  $d^3$  configuration.<sup>57</sup> The counter cation ( $\text{K}^+$ ) can be fully-exchanged with other alkali metal cations in aqueous solutions, and the states of water molecules in the channels can be controlled by the type of alkali metal ions:<sup>58</sup> alkali metal ions with high ionic potentials (e.g.,  $\text{Li}^+$ ) form dense and extensive hydrogen-bonding network of water molecules with mobile protons at the periphery, which leads to high proton conductivities of  $10^{-3} \text{ S cm}^{-1}$  without any acidic functional groups (Fig. 6).<sup>58</sup>

#### 4. Reduction-induced cation-uptake in polyoxometalate-based ionic solids

Redox property of solids is a key for selective cation-uptake and exchange relevant to material science. For example, Yoshikawa, Awaga, and co-workers have reported that  $\alpha$ -Keggin-type phosphododecamolybdate  $[\alpha\text{-PMo}_{12}\text{O}_{40}]^{3-}$  exhibits reversible 24-electron redox during charging/discharging due to the twelve molybdenum atoms ( $\text{Mo}^{(\text{IV/VI})}$ ) coupled with  $\text{Li}^+$  uptake/release, as a component of molecular cluster battery.<sup>59</sup> Therefore, it can be suggested that one of the best way to engineer redox-active porous solids would be to incorporate redox-active components. A landmark example was reported by Cronin and co-workers: a porous solid composed of silicodectungstate  $[\gamma\text{-SiW}_{10}\text{O}_{36}]^{8-}$  and  $\text{Mn}^{3+}$  was synthesized, and the oxidation

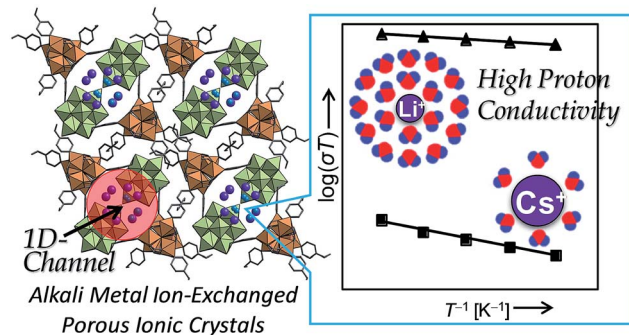


Fig. 6 (Left) Crystal structure of  $\text{K}_2[\text{Cr}_3\text{O}(\text{OOCH})_6(4\text{-methylpyridine})_3]_2[\alpha\text{-SiW}_{12}\text{O}_{40}] \cdot n\text{H}_2\text{O}$ . Light green and orange polyhedra show the  $[\text{WO}_6]$  and  $[\text{Cr}_3\text{O}_6\text{N}]$  units, respectively. Purple and blue spheres show the alkali metal ions and oxygen atoms of the water of crystallization, respectively. (Right) Arrhenius plots of the temperature dependent proton conductivities at RH 95% (303–323 K). Proton conductivities of the compound with  $\text{Li}^+$  and  $\text{Cs}^+$  as counter cations were  $1.9 \times 10^{-3}$  and  $1.2 \times 10^{-7} \text{ S cm}^{-1}$ , respectively (323 K).<sup>58</sup>

states of  $\text{Mn}^{(\text{II/III})}$  can be switched by the addition of reducing/oxidizing reagents.<sup>60</sup> They have later synthesized another redox-active porous solid with cyclic POM  $[\text{P}_8\text{W}_{48}\text{O}_{148}]^{40-}$  units and  $\text{Mn}^{(\text{II/III})}$  (Fig. 7), and the cation-exchange rate and capacity can be controlled by the oxidation states of  $\text{Mn}$ .<sup>61</sup>

We have reported a redox-active porous ionic crystal  $\text{A}[\text{Cr}_3\text{O}(\text{OOCH})_6(4\text{-methylpyridine})_3]_2[\alpha\text{-PMo}_{12}\text{O}_{40}] \cdot n\text{H}_2\text{O}$  ( $\text{A}$  = alkali metal ions) possessing one-dimensional channels, and the treatment of the crystal with reducing (ascorbic acid) or oxidizing (chlorine water) reagents results in one-electron redox of the POM ( $\text{Mo}^{(\text{V/VI})}$ ) coupled with uptake/release of alkali metal ions, and the reaction rate depended on the type of alkali metal ions.<sup>62</sup> The reaction rate increased in the order of  $\text{K}^+ < \text{Rb}^+ < \text{Cs}^+$ , which is in line with the order of hydration radius and dehydration enthalpy of the cations (Fig. 1).<sup>44,62</sup> This work was extended by the utilization of  $[\alpha\text{-SiMo}_{12}\text{O}_{40}]^{4-}$ , which resulted in the formation of an ionic crystal with isolated pores instead of continuous one-dimensional ones (Fig. 8).<sup>63</sup> The compound selectively adsorbed  $\text{Cs}^+$  among alkali and alkaline earth metal ions *via* reduction of the POM in the compound with ascorbic acid, showing potential applicability as an adsorbent for radioactive  $\text{Cs}^+$  removal from environmental water. Despite the high selectivity to  $\text{Cs}^+$ , there were several tasks to solve: requirement of heating (343 K) and slow adsorption kinetics (12 h to reach equilibrium). In order to solve these tasks, large-molecular size and easily reducible Wells-Dawson-type POMs  $[\alpha\text{-P}_2\text{M}_{18}\text{O}_{62}]^{6-}$  ( $\text{M}$  = Mo, W) were utilized to increase the pore volume and to facilitate the reduction-induced  $\text{Cs}^+$  uptake.<sup>64</sup> As expected,  $\text{Cs}^+$ -uptake capacity and rate increased largely (only 1 h to reach equilibrium at room temperature).

Metal clusters are a topic of great interest in materials science and have found numerous applications especially in catalysis and electro-optics.<sup>65</sup> Microporous compounds offer versatile scaffolds for the formation and stabilization of metal clusters from metal ions. For example, small mixed-valence silver clusters have been synthesized in zeolites by calcination of  $\text{Ag}^{+}$ -exchanged zeolites at high temperature:  $\text{Ag}_4^{2+}$  in MFI-



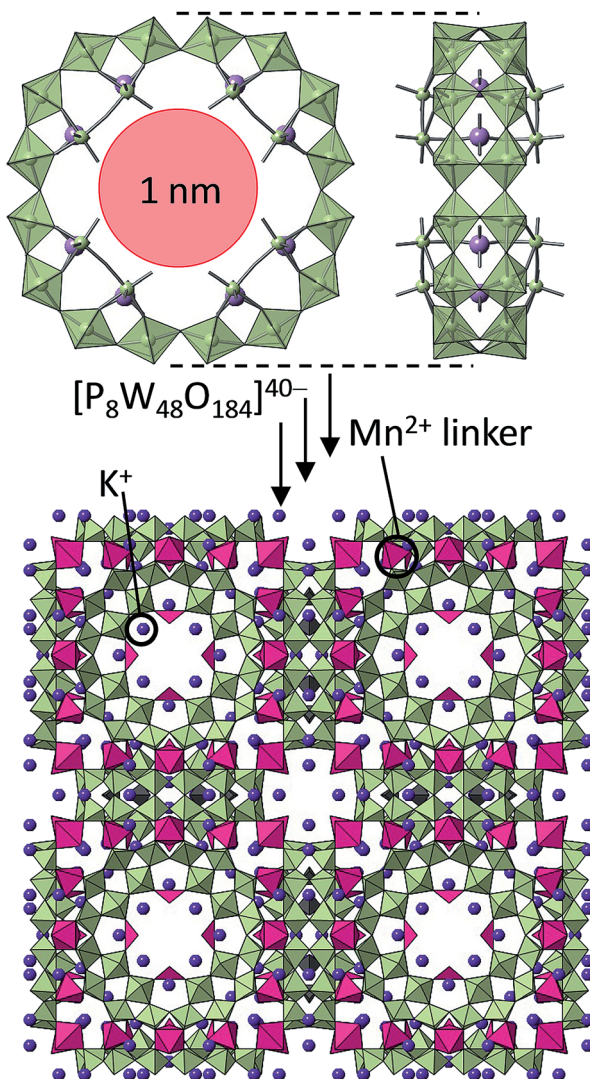


Fig. 7 (Upper) Molecular structure of  $[P_8W_{48}O_{184}]^{40-}$  comprising a nanometer-size cavity. (Lower) The molecular unit is linked by  $Mn^{2+}$  resulting in a 3D-POM framework.<sup>51</sup>

zeolite<sup>66</sup> is active for the selective reduction of NO by propane with  $O_2$  and  $H_2$ , and  $Ag^{2+}$  in LTA-zeolite<sup>67</sup> shows on-off switching of yellow-green photoluminescence (PL) by hydration-dehydration. A landmark report on formation of metal clusters in redox-active MOFs has been carried out by reducing  $Pd^{2+}$  *via* electron transfer from nitrilotrisbenzoate, which is a redox-active organic linker of the porous framework.<sup>68</sup> However, redox of MOFs is mostly limited to the utilization of redox-active organic ligands because redox of the metal center ion induces large change in the coordination geometry causing to collapse the porous framework. Therefore, metal clusters in MOFs have been synthesized by adding reducing reagents such as  $H_2$ ,  $NaBH_4$ ,  $DMF$ , *etc.*<sup>69-71</sup> to the MOF comprising metal ions, and homogeneous formation and distribution of metal clusters become a problem.

As explained above, POMs can store multiple electrons in the molecular framework and have been utilized as constituents of redox-active porous frameworks. Some compounds show

cooperative migration of electrons with metal ions,<sup>61-64</sup> so called cation-coupled electron-transfer (CCET) in relation to proton-coupled electron-transfer<sup>72</sup> (PCET). Quite recently, we have utilized redox-active porous ionic crystals  $Cs[Cr_3O(OOCH)_6(4\text{-methylpyridine})_3]_2[\alpha\text{-PMo}_{12}^{VI}O_{40}] \cdot nH_2O$  (**Cs-ox**) and  $Cs_2[Cr_3O(OOCH)_6(4\text{-methylpyridine})_3]_2[\alpha\text{-PMo}_{11}^{VI}Mo^{V}O_{40}] \cdot nH_2O$  (**Cs<sub>2</sub>-red**) (the abbreviations **Cs-ox** and **Cs<sub>2</sub>-red** are based on the types and numbers of counter cations and the oxidation state of POM), to form and stabilize small mixed-valence luminescent silver clusters in the one-dimensional channel (Fig. 9). According to elemental analysis of cesium and silver in the compounds by atomic absorption spectrometry (AAS), we have found that reduction-induced ion-exchange of  $Cs^+$  in **Cs<sub>2</sub>-red** with  $Ag^+$  from  $AgNO_3(aq.)$ , and subsequent formation of a mixed-valence luminescent silver cluster  $Ag_4^{2+}$  took <1 min (eqn (5)), while the simple ion-exchange with  $Cs^+$  in **Cs-ox** with  $Ag^+$  from  $AgNO_3(aq.)$  took >24 h (eqn (6)):<sup>73</sup>

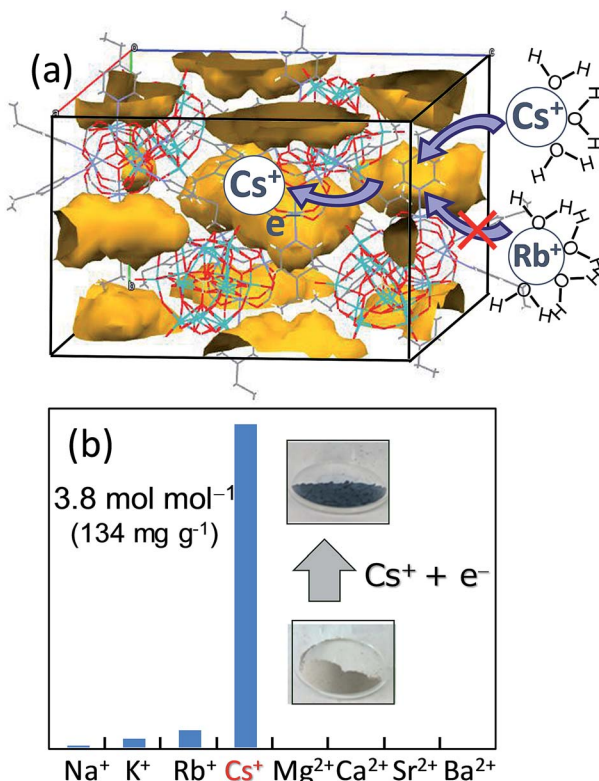
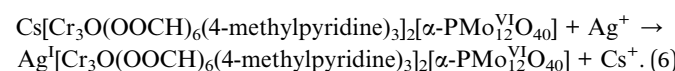
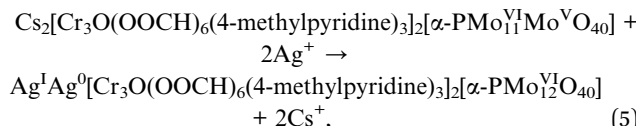


Fig. 8 (a) Crystal structure of  $(etpyH)_2[Cr_3O(OOCH)_6(etpy)_3]_2[\alpha\text{-SiMo}_{12}O_{40}] \cdot nH_2O$  (etpy = 4-ethylpyridine). Each void (in yellow-brown) has a size of ca.  $6.5 \text{ \AA} \times 12.5 \text{ \AA}$ . (b) Amounts of cations incorporated by the reduction-induced method. Note that there is a color change due to the reduction of POM upon  $Cs^+$  uptake.<sup>63</sup>

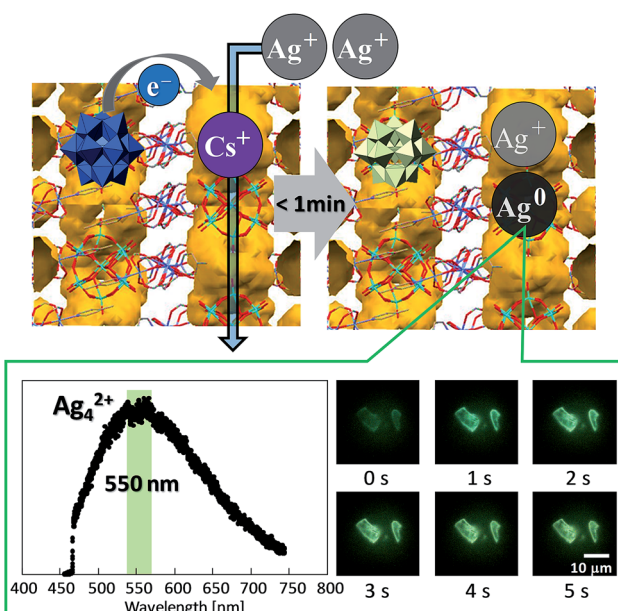


Fig. 9 Schematic illustration of the reduction-induced ion-exchange of  $\text{Cs}^+$  with  $\text{Ag}^+$  in the one-dimensional channel (in yellow-brown) to form small mixed-valence luminescent silver clusters. PL spectrum and time course of PL images of a single crystal of  $\text{Cs}_2\text{-red}$  in  $\text{AgNO}_3(\text{aq})$  (excitation at 405 nm).<sup>73</sup>

Note that the formation of  $\text{Ag}_4^{2+}$  in the redox-active porous ionic crystals was assumed according to the report that  $\text{Ag}_4^{2+}$  in LTA-zeolite emits yellow-green light giving a broad emission band around 550 nm.<sup>67</sup> According to the PL images in Fig. 9,  $\text{Ag}_4^{2+}$  is formed within few seconds. A model fitting of the time course of PL intensity has shown that the reduction-induced ion-exchange consists of two steps: electron transfer from the reduced POM ( $[\alpha\text{-PMo}_{11}^{\text{VI}}\text{Mo}^{\text{V}}\text{O}_{40}]^{4-}$ ) to  $\text{Ag}^+$  and subsequent formation of a silver cluster  $\text{Ag}_4^{2+}$ , and diffusion of the silver cluster and exchange with  $\text{Cs}^+$ . The compound containing the silver cluster showed high affinity toward unsaturated hydrocarbon guests (acetylene and ethylene).  $\text{Ag}/\text{Al}_2\text{O}_3$  has been commercialized as a catalyst for the epoxidation of ethylene and propylene, and small mixed-valence silver clusters have been suggested as the activation site of this reaction.<sup>74</sup> Our next aim is to form and stabilize these clusters in redox-active ionic crystals with mesopores, and to apply them as solid catalysts. In addition, synthesis of metal clusters with different elements, sizes, and charges by controlling the pore size and degree of reduction of the POM-based redox-active scaffold is currently under investigation.

## 5. Summary and outlook

In this perspective, cation-uptake and exchange in POMs and POM-based compounds were categorized and reviewed in three groups. (i) POMs as inorganic crown ethers and cryptands: POMs can offer versatile platforms for cation coordination, which are different from those of the organic counterparts, and one of the next targets would be to substitute oxygen ( $\text{O}^{2-}$ ) of

POMs with sulfur ( $\text{S}^{2-}$ ), selenium ( $\text{Se}^{2-}$ ), etc.<sup>75</sup> to tune the coordination environment. (ii) POM-based ionic solids as cation-exchangers: the next target would be to explore cooperative effects of the selectively adsorbed cations and POMs,<sup>55</sup> especially as optical materials, magnetic materials, solid catalysts, etc. (iii) Reduction-induced cation-uptake in POM-based ionic solids: while it is difficult for conventional porous compounds such as zeolites and MOFs to support the geometry change in the framework that often accompany the redox processes, POM-based solids show great potential for the multiple and reversible uptake/release of cations with electrons.<sup>60-64,73</sup> Such CCET reactions in solids can be applied not only to selective cation-uptake and sensing but also to the next-generation rechargeable batteries,<sup>76</sup> solid catalysts for water splitting, chemical fixation of  $\text{CO}_2$ , ammonia synthesis, etc.

Another challenge is anion-exchange in POM-based compounds. This notion includes substitution of  $\text{O}^{2-}$  in POMs with  $\text{S}^{2-}$ ,  $\text{Se}^{2-}$ ,  $\text{N}^{3-}$  or halide ions as well as incorporation of multiple types of anions in the ionic solid. A recent review on metal oxyfluorides and oxynitrides show that incorporation of multiple anions in metal oxide-based compounds can finely modulate physicochemical properties such as catalysis, optics, conduction, magnetism, etc.<sup>77</sup> Some MOFs with cationic frameworks show anion-exchange properties,<sup>78</sup> according to the Hofmeister series<sup>79</sup> (citrate (trivalent) > sulfate (divalent) > acetate (monovalent) >  $\text{HCO}_3^-$  >  $\text{Cl}^-$  >  $\text{Br}^-$  >  $\text{I}^-$  >  $\text{NO}_3^-$ , which is in line with the degree of hydration) or non-Hofmeister selectivity due to the utilization of Lewis acid and/or multidentate donors.<sup>80</sup> We have recently reported the synthesis of cesium salts of  $\alpha$ -Keggin-type  $[\alpha\text{-BW}_{12}\text{O}_{40}]^{5-}$  (BW) and  $[\alpha\text{-SiW}_{12}\text{O}_{40}]^{4-}$  (SiW) blends, and the porosity is finely controlled by the BW/SiW ratio.<sup>81</sup> The next aim would be to synthesize these mixed-POM compounds post-synthetically or by anion-exchange.

## Conflicts of interest

There are no conflicts to declare.

## Acknowledgements

This work was supported by JST-PRESTO (JPMJPR1312) and grant-in-aids for scientific research JP16K05742, JP19H04564 (Coordination Asymmetry), and JP19H04686 (Mixed Anion) from MEXT of Japan. Prof. N. Mizuno (Univ. of Tokyo) is acknowledged for his continuous encouragement and support on this research. Collaborators, and former and current students of Uchida group are acknowledged for their contribution on this research.

## Notes and references

1. A. Clearfield, Role of ion exchange in solid-state chemistry, *Chem. Rev.*, 1988, **88**, 125–148.
2. J. B. Rivest and P. K. Jain, Cation exchange on the nanoscale: an emerging technique for new material synthesis, device fabrication, and chemical sensing, *Chem. Soc. Rev.*, 2013, **42**, 89–96.



3 J. P. Morth, B. P. Pedersen, M. S. Toustrup-Jensen, T. L. M. Sørensen, J. Petersen, J. P. Andersen, B. Vilsen and P. Nissen, Crystal structure of the sodium-potassium pump, *Nature*, 2007, **450**, 1043–1049.

4 C. J. Pedersen, Cyclic polyethers and their complexes with metal salts, *J. Am. Chem. Soc.*, 1967, **89**, 7017–7036.

5 G. W. Gokel, W. M. Leevy and M. E. Weber, Crown ethers: Sensors for ions and molecular scaffolds for materials and biological models, *Chem. Rev.*, 2004, **104**, 2723–2750.

6 M. E. Davis and R. F. Lobo, Zeolite and Molecular Sieve Synthesis, *Chem. Mater.*, 1992, **4**, 756–768.

7 D. W. Breck, W. G. Eversole, R. M. Milton, T. B. Reed and T. L. Thomas, Crystalline zeolites. I. The properties of a new synthetic zeolite, type A, *J. Am. Chem. Soc.*, 1956, **78**, 5963–5972.

8 O. Talu, S. Y. Zhang and D. T. Hayhurst, Effect of cations on methane adsorption by NaY, MgY, CaY, SrY, and BaY zeolites, *J. Phys. Chem.*, 1993, **97**, 12894–12898.

9 O. M. Dzhigit, A. V. Kiselev, K. N. Mikos, G. G. Muttik and T. A. Rahmanova, Heats of adsorption of water vapour on X-zeolites containing  $\text{Li}^+$ ,  $\text{Na}^+$ ,  $\text{K}^+$ ,  $\text{Rb}^+$ , and  $\text{Cs}^+$  cations, *Trans. Faraday Soc.*, 1971, **67**, 458–467.

10 M. Dincă and J. R. Long, High-enthalpy hydrogen adsorption in cation-exchanged variants of the microporous metal-organic framework  $\text{Mn}_3[(\text{Mn}_4\text{Cl})_3(\text{BTT})_8(\text{CH}_3\text{OH})_{10}]_2$ , *J. Am. Chem. Soc.*, 2007, **129**, 11172–11176.

11 C. K. Brozek and M. Dincă, Cation exchange at the secondary building units of metal-organic frameworks, *Chem. Soc. Rev.*, 2014, **43**, 5456–5467.

12 B. J. Beberwyck, Y. Surendranath and A. P. Alivisatos, Cation Exchange: A versatile tool for nanomaterials synthesis, *J. Phys. Chem. C*, 2013, **117**, 19759–19770.

13 X. Liu, G. B. Braun, M. Qin, E. Ruoslahti and K. N. Sugahara, In vivo cation exchange in quantum dots for tumor-specific imaging, *Nat. Commun.*, 2017, **8**, 343.

14 M. T. Pope, *Heteropoly and Isopoly Oxometalates*, Springer-Verlag, New York, 1983.

15 M. T. Pope and A. Müller, Polyoxometalate chemistry: An old field with new dimensions in several disciplines, *Angew. Chem., Int. Ed. Engl.*, 1991, **30**, 34–48.

16 C. L. Hill, Thematic issue on polyoxometalate, *Chem. Rev.*, 1998, **98**, 1–390.

17 L. Cronin and A. Müller, From serendipity to design of polyoxometalates at the nanoscale, aesthetic beauty and applications, *Chem. Soc. Rev.*, 2012, **41**, 7325–7648.

18 E. Coronado, C. Giménez-Saiz and C. J. Gómez-García, Recent advances in polyoxometalate-containing molecular conductors, *Coord. Chem. Rev.*, 2005, **249**, 1776–1796.

19 A. Proust, R. Thouvenot and P. Gouzerh, Functionalization of polyoxometalates: towards advanced applications in catalysis and materials science, *Chem. Commun.*, 2008, 1837–1852.

20 D. Li, P. Yin and T. Liu, Supramolecular architectures assembled from amphiphilic hybrid polyoxometalates, *Dalton Trans.*, 2012, **41**, 2853–2861.

21 K. Y. Monakhov, W. Bensch and P. Kögerler, Semimetal-functionalized polyoxovanadates, *Chem. Soc. Rev.*, 2015, **44**, 8443–8483.

22 K. Suzuki, N. Mizuno and K. Yamaguchi, Polyoxometalate photocatalysis for liquid-phase selective organic functional group transformations, *ACS Catal.*, 2018, **8**, 10809–10825.

23 P. Yang and U. Kortz, Discovery and evolution of polyoxopalladates, *Acc. Chem. Res.*, 2018, **51**, 1599–1608.

24 I. A. Weinstock, R. E. Schreiber and R. Neumann, Dioxygen in polyoxometalate mediated reactions, *Chem. Rev.*, 2018, **118**, 2680–2717.

25 L. Chen, W.-L. Chen, X.-L. Wang, Y.-G. Li, Z.-M. Su and E.-B. Wang, Polyoxometalates in dye-sensitized solar cells, *Chem. Soc. Rev.*, 2019, **48**, 260–284.

26 V. Pekárek and V. Veselý, Synthetic inorganic ion exchangers-II: Salts of heteropolyacids, insoluble ferrocyanides, synthetic aluminosilicates and miscellaneous exchangers, *Talanta*, 1972, **19**, 1245–1283.

27 B. Dietrich, J. M. Lehn and J. P. Sauvage, Diaza-polyoxamacrocycles et macrobicycles, *Tetrahedron Lett.*, 1969, **34**, 2885–2889.

28 B. Dietrich, J. M. Lehn and J. P. Sauvage, Les cryptates, *Tetrahedron Lett.*, 1969, **34**, 2889–2892.

29 W. G. Klemperer and G. Westwood, Traps for cations, *Nat. Mater.*, 2003, **2**, 780–781.

30 F. Robert, M. Leyrie, G. Hervé, A. Tézé and Y. Jeannin, Crystal structure of ammonium dicobalto(II)-40-tungstotetraarsenate(III). Allosteric effects in the ligand, *Inorg. Chem.*, 1980, **19**, 1746–1752.

31 B. Kandasamy, T. Sudmeier, W. W. Ayass, Z. Lin, Q. Feng, B. S. Bassil and U. Kortz, Selective  $\text{Rb}^+$  vs.  $\text{K}^+$  guest incorporation in wheel-shaped 27-tungsto-3-arsenate(III) host,  $[\text{M} \subset \{(\beta\text{-As}^{\text{III}}\text{W}_8\text{O}_{30})(\text{WO}(\text{H}_2\text{O}))\}_3]^{14-}$  ( $\text{M} = \text{K}, \text{Rb}$ ), *Eur. J. Inorg. Chem.*, 2019, 502–505.

32 M. H. Alizadeh, S. P. Harmalkar, Y. Jeannin, J. Martin-Frere and M. T. Pope, A heteropolyanion with fivefold molecular symmetry that contains a nonlabile encapsulated sodium ion. The structure and chemistry of  $[\text{NaP}_5\text{W}_{30}\text{O}_{110}]^{14-}$ , *J. Am. Chem. Soc.*, 1985, **107**, 2662–2669.

33 I. Greaser, M. C. Heckel, R. J. Neitz and M. T. Pope, Rigid nonlabile polyoxometalate cryptates  $[\text{ZP}_5\text{W}_{30}\text{O}_{110}]^{(15-n)-}$  that exhibit unprecedented selectivity for certain lanthanide and other multivalent cations, *Inorg. Chem.*, 1993, **32**, 1573–1578.

34 J. A. Fernández, X. López, C. Bo, C. de Graaf, E. J. Baerends and J. M. Poblet, Polyoxometalates with internal cavities: redox activity, basicity and cation encapsulation in  $[\text{X}^{n+}\text{P}_5\text{W}_{30}\text{O}_{110}]^{(15-n)-}$  Preyssler Complexes, with  $\text{X} = \text{Na}^+$ ,  $\text{Ca}^{2+}$ ,  $\text{Y}^{3+}$ ,  $\text{La}^{3+}$ ,  $\text{Ce}^{3+}$ , and  $\text{Th}^{4+}$ , *J. Am. Chem. Soc.*, 2007, **129**, 12244–12253.

35 Z.-M. Zhang, S. Yao, Y.-G. Li, X.-B. Han, Z.-M. Su, Z.-S. Wang and E.-B. Wang, Inorganic crown ethers: Sulfate-based Preyssler polyoxometalates, *Chem.-Eur. J.*, 2012, **18**, 9184–9188.

36 A. Müller, S. K. Das, S. Talismanov, S. Roy, E. Beckmann, H. Bögge, M. Schmidtmann, A. Merca, A. Berkle, L. Allouche, Y. Zhou and L. Zhang, Trapping cations in specific positions in tunable “artificial cell” channels: New nanochemistry perspectives, *Angew. Chem., Int. Ed.*, 2003, **42**, 5039–5044.



37 A. Müller, D. Rehder, E. T. K. Haupt, A. Merca, H. Bögge, M. Schmidtmann and G. Heinze-Brückner, Artificial cells: Temperature-dependent, reversible  $\text{Li}^+$ -ion uptake/release equilibrium at metal oxide nanocontainer pores, *Angew. Chem., Int. Ed.*, 2004, **43**, 4466–4470.

38 A. Müller, L. Toma, H. Bögge, C. Schäffer and A. Stammmer, Porous capsules allow pore opening and closing that results in cation uptake, *Angew. Chem., Int. Ed.*, 2005, **44**, 7757–7761.

39 A. Yoshida, Y. Nakagawa, K. Uehara, S. Hikichi and N. Mizuno, Inorganic cryptand: Size-selective strong metallic cation encapsulation by a disilicoicosatungstate ( $\text{Si}_2\text{W}_{20}$ ) polyoxometalate, *Angew. Chem., Int. Ed.*, 2009, **48**, 7055–7058.

40 V. Baskar, M. Shanmugam, M. Helliwell, S. J. Teat and R. E. P. Winpenny, Reverse-Keggin ions: Polycondensation of antimonate ligands give inorganic cryptand, *J. Am. Chem. Soc.*, 2007, **129**, 3042–3043.

41 M. Barsukova, N. V. Izarova, R. N. Biboum, B. Keita, L. Nadjo, V. Ramachandran, N. S. Dalal, N. S. Antonova, J. J. Carbó, J. M. Poblet and U. Kortz, Polyoxopalladates encapsulating yttrium and lanthanide ions  $[\text{X}^{\text{III}}\text{Pd}_{12}^{\text{II}}(\text{AsPh})_8\text{O}_{32}]^{5-}$  ( $\text{X} = \text{Y, Pr, Nd, Sm, Eu, Gd, Tb, Dy, Ho, Er, Tm, Yb, Lu}$ ), *Chem.-Eur. J.*, 2010, **16**, 9076–9085.

42 M. Barsukova-Stuckart, N. V. Izarova, R. A. Barrett, Z. Wang, J. van Tol, H. W. Kroto, N. S. Dalal, P. Jiménez-Lozano, J. J. Carbó, J. M. Poblet, M. S. von Gernler, T. Drewello, P. de Oliveira, B. Keita and U. Kortz, Polyoxopalladates encapsulating 8-coordinated metal ions,  $[\text{MO}_8\text{Pd}_{12}^{\text{II}}\text{L}_8]^{n-}$  ( $\text{M} = \text{Sc}^{3+}, \text{Mn}^{2+}, \text{Fe}^{3+}, \text{Co}^{2+}, \text{Ni}^{2+}, \text{Cu}^{2+}, \text{Zn}^{2+}, \text{Lu}^{3+}; \text{L} = \text{PhAsO}_3^{2-}, \text{PhPO}_3^{2-}, \text{SeO}_3^{2-}$ ), *Inorg. Chem.*, 2012, **51**, 13214–13228.

43 P. Yang, Y. Xiang, Z. Lin, B. S. Bassil, J. Cao, L. Fan, Y. Fan, M.-X. Li, P. Jiménez-Lozano, J. J. Carbó, J. M. Poblet and U. Kortz, Alkaline earth guests in polyoxopalladate chemistry: From nanocube to nanostar via an open-shell structure, *Angew. Chem., Int. Ed.*, 2014, **53**, 11974–11978.

44 W. R. Fawcett, Thermodynamic parameters for the solvation of monatomic ions in water, *J. Phys. Chem. B*, 1999, **103**, 11181–11185.

45 M. Nyman, J. P. Larentzos, E. J. Maginn, M. E. Welk, D. Ingersoll, H. Park, J. B. Parise, I. Bull and F. Bonhomme, Experimental and theoretical methods to investigate extraframework species in a layered material of dodecaniobate anions, *Inorg. Chem.*, 2007, **46**, 2067–2079.

46 M. Nyman, C. R. Powers, F. Bonhomme, T. M. Alam, E. J. Maginn and D. T. Hobbs, Ion-exchange behavior of one-dimensional linked dodecaniobate Keggin ion materials, *Chem. Mater.*, 2008, **20**, 2513–2521.

47 Z. Zhang, M. Sadakane, T. Murayama, N. Sakaguchi and W. Ueda, Preparation, structural characterization, and ion-exchange properties of two new zeolite-like 3D frameworks constructed by  $\epsilon$ -Keggin-type polyoxometalates with binding metal ions,  $\text{H}_{11.4}[\text{ZnMo}_{12}\text{O}_{40}\text{Zn}_2]^{1.5-}$  and  $\text{H}_{7.5}[\text{Mn}_{0.2}\text{Mo}_{12}\text{O}_{40}\text{Mn}_2]^{2.1-}$ , *Inorg. Chem.*, 2014, **53**, 7309–7318.

48 Z. Zhang, T. Murayama, M. Sadakane, H. Ariga, N. Yasuda, N. Sakaguchi, K. Asakura and W. Ueda, *Nat. Commun.*, 2015, **6**, 7731.

49 Q. Zhu, Z. Zhang, M. Sadakane, A. Yoshida, M. Hara and W. Ueda, Synthesis of crystalline molybdenum oxides based on a 1D molecular structure and their ion-exchange properties, *New J. Chem.*, 2017, **41**, 4503–4509.

50 T. Okuhara, H. Watanabe, T. Nishimura, K. Inumaru and M. Misono, Microstructure of cesium hydrogen salts of 12-tungstophosphoric acid relevant to novel acid catalysis, *Chem. Mater.*, 2000, **12**, 2230–2238.

51 T. Okuhara, Water-tolerant solid acid catalysts, *Chem. Rev.*, 2002, **102**, 3641–3666.

52 Y. Iwase, S. Sano, L. Mahardiani, R. Abe and Y. Kamiya, Bimodal cesium hydrogen salts of 12-tungstosilicic acid,  $\text{Cs}_x\text{H}_{4-x}\text{SiW}_{12}\text{O}_{40}$ , as highly active solid acid catalysts for transesterification of glycerol tributyrate with methanol, *J. Catal.*, 2014, **318**, 34–42.

53 K. Okamoto, S. Uchida, T. Ito and N. Mizuno, Self-organization of all-inorganic dodecatungstophosphate nanocrystallites, *J. Am. Chem. Soc.*, 2007, **129**, 7378–7384.

54 Y. Ogasawara, S. Uchida, T. Maruichi, R. Ishikawa, N. Shibata, Y. Ikuhara and N. Mizuno, Cubic cesium hydrogen silicododecatungstate with anisotropic morphology and polyoxometalate vacancies exhibiting selective water sorption and cation-exchange properties, *Chem. Mater.*, 2013, **25**, 905–911.

55 D.-D. Zhou, Q. Zhao, F.-P. Zhu, Z.-G. Zhang, Y. Zhou, Z.-J. Yong, J.-P. Ma, Y. Kuroiwa, C. Moriyoshi, Y.-Z. Fang, J.-L. Gu, J. Shu, Z.-Y. Li, J.-M. Chen, L.-R. Zheng and H.-T. Sun, Ion-exchangeable microporous polyoxometalate compounds with off-center dopants exhibiting unconventional luminescence, *Chem.-Eur. J.*, 2018, **24**, 9976–9982.

56 S. Uchida, R. Eguchi and N. Mizuno, Zeotype organic-inorganic ionic crystals: Facile cation exchange and controllable sorption properties, *Angew. Chem., Int. Ed.*, 2010, **49**, 9930–9934.

57 T. Fujihara, J. Aonahata, S. Kumakura, A. Nagasawa, K. Murakami and T. Ito, Kinetic study on the substitution of dimethylacetamide for the terminal aqua ligands in the trinuclear chromium(III) complexes  $[\text{Cr}_3(\mu_3\text{O})(\mu\text{-RCO}_2)_6(\text{H}_2\text{O})_3]^+$  ( $\text{R} = \text{H, CH}_3, \text{CH}_3\text{CH}_2, \text{CH}_2\text{Cl, CHCl}_2, \text{CH}_3\text{OCH}_2, (\text{CH}_3)_3\text{C, CH}_2\text{ClCH}_2, (\text{CH}_3\text{CH}_2)_2\text{CH}$ ). Elucidation of the mechanism from the activation volumes and the substituent effects of bridging carboxylate ligands, *Inorg. Chem.*, 1998, **37**, 3779–3784.

58 S. Uchida, R. Hosono, R. Eguchi, R. Kawahara, R. Osuga, J. N. Kondo, M. Hibino and N. Mizuno, Proton conduction in alkali metal ion-exchanged porous ionic crystals, *Phys. Chem. Chem. Phys.*, 2017, **19**, 29077–29083.

59 H. Wang, S. Hamanaka, Y. Nishimoto, S. Irle, T. Yokoyama, H. Yoshikawa and K. Awaga, In operando X-ray absorption fine structure studies of polyoxometalate molecular cluster batteries: Polyoxometalates as electron sponges, *J. Am. Chem. Soc.*, 2012, **134**, 4918–4924.

60 C. Ritchie, C. Streb, J. Thiel, S. G. Mitchell, H. N. Miras, D.-L. Long, T. Boyd, R. D. Peacock, T. McGlone and L. Cronin, Reversible redox reactions in and extended



polyoxometalate framework solid, *Angew. Chem., Int. Ed.*, 2008, **47**, 6881–6884.

61 S. G. Mitchell, C. Streb, H. N. Miras, T. Boyd, D.-L. Long and L. Cronin, Face-directed self-assembly of an electronically active Archimedean polyoxometalate architecture, *Nat. Chem.*, 2010, **2**, 308–312.

62 R. Kawahara, S. Uchida and N. Mizuno, Redox-induced reversible uptake-release of cations in porous ionic crystals based on polyoxometalate: Cooperative migration of electrons with alkali metal ions, *Chem. Mater.*, 2015, **27**, 2092–2099.

63 S. Seino, R. Kawahara, Y. Ogasawara, N. Mizuno and S. Uchida, Reduction-induced highly selective uptake of  $\text{Cs}^+$  by an ionic crystal based on silicododecamolybdate, *Angew. Chem., Int. Ed.*, 2016, **55**, 3987–3991.

64 S. Hitose and S. Uchida, Rapid uptake/release of  $\text{Cs}^+$  in isostructural redox-active porous ionic crystals with large molecular size and easily reducible Dawson-type polyoxometalates as building blocks, *Inorg. Chem.*, 2018, **57**, 4833–4836.

65 E. C. Tyo and S. Vajda, Catalysis by clusters with precise numbers of atoms, *Nat. Nanotechnol.*, 2015, **10**, 577–588.

66 J. Shibata, K. Shimizu, Y. Takada, A. Shichi, H. Yoshida, S. Satokawa, A. Satsuma and T. Hattori, Structure of active Ag clusters in Ag zeolites for SCR of NO by propane in the presence of hydrogen, *J. Catal.*, 2004, **227**, 367–374.

67 S. Aghakhani, D. Grandjean, W. Baekelant, E. Coutiño-Gonzalez, E. Fron, K. Kvashnina, M. B. J. Roeffaers, J. Hofkens, B. F. Sels and P. Lievens, *Nanoscale*, 2018, **10**, 11467–11476.

68 Y. E. Cheon and M. P. Suh, Enhanced hydrogen storage by palladium nanoparticles fabricated in a redox-active metal–organic framework, *Angew. Chem., Int. Ed.*, 2009, **48**, 2899–2903.

69 H. L. Jiang, T. Akita, T. Ishida, M. Haruta and Q. Xu, Synergistic catalysis of Au@Ag core–shell nanoparticles stabilized on metal–organic framework, *J. Am. Chem. Soc.*, 2011, **133**, 1304–1306.

70 H. Liu, L. Chang, L. Chen and Y. Li, In situ one-step synthesis of metal–organic framework encapsulated naked Pt nanoparticles without additional reductants, *J. Mater. Chem. A*, 2015, **3**, 8028–8033.

71 H. Liu, L. Chang, C. Bai, L. Chen, R. Luque and Y. Li, Controllable encapsulation of “clean” metal clusters within MOFs through kinetic modulation: towards advanced heterogeneous nanocatalysts, *Angew. Chem., Int. Ed.*, 2016, **55**, 5019–5023.

72 J. J. Warren, T. A. Tronic and J. M. Mayer, Thermochemistry of proton-coupled electron transfer reagents and its implications, *Chem. Rev.*, 2010, **110**, 6961–7001.

73 S. Uchida, T. Okunaga, Y. Harada, S. Magira, Y. Noda, T. Mizuno and T. Tachikawa, Rapid formation of small mixed-valence luminescent silver clusters via cation-coupled electron-transfer in redox-active porous ionic crystal based on dodecamolybdate, *Nanoscale*, 2019, **11**, 5460–5466.

74 Y. Lei, F. Mehmood, J. Greeley, B. Lee, S. Seifert, R. E. Winans, J. W. Elam, R. J. Meyer, P. C. Redfern, D. Teschner, R. Schlögl, M. J. Pellin, L. A. Curtiss and S. Vajda, Increased silver activity for direct propylene epoxidation via subnanometer size effects, *Science*, 2010, **328**, 224–228.

75 E. Cadot, B. Salignac, T. Loiseau, A. Dolbecq and F. Sécheresse, Syntheses and  $^{31}\text{P}$  NMR studies of cyclic oxothiomolybdate(v) molecular rings: Exchange properties and crystal structures of the monophosphate decamer  $[(\text{H}_2\text{PO}_4)\text{Mo}_{10}\text{S}_{10}\text{O}_{10}(\text{OH})_{11}(\text{H}_2\text{O})_2]^{2-}$  and the diphosphate dodecamer  $[(\text{HPO}_4)_2\text{Mo}_{12}\text{S}_{12}\text{O}_{12}(\text{OH})_{12}(\text{H}_2\text{O})_2]^{4-}$ , *Chem.–Eur. J.*, 1999, **5**, 3390–3398.

76 Y. Ji, L. Huang, J. Hu, C. Streb and Y.-F. Song, Polyoxometalate-functionalized nanocarbon materials for energy conversion, energy storage and sensor systems, *Energy Environ. Sci.*, 2015, **8**, 776–789.

77 H. Kageyama, K. Hayashi, K. Maeda, J. P. Attfield, Z. Hiroi, J. M. Rondinelli and K. R. Poeppelmeier, Expanding frontiers in materials chemistry and physics with multiple anions, *Nat. Commun.*, 2018, **9**, 772.

78 B. F. Hoskins and R. Robson, Design and construction of a new class of scaffolding-like materials comprising infinite polymeric frameworks of 3D-linked molecular rods. A reappraisal of the zinc cyanide and cadmium cyanide structures and the synthesis and structure of the diamond-related frameworks  $[\text{N}(\text{CH}_3)_4][\text{Cu}^{\text{I}}\text{Zn}^{\text{II}}(\text{CN})_4]$  and  $\text{Cu}^{\text{I}}[4,4',4'',4''\text{-tetracyanotetraphenylmethane}] \text{BF}_4 \cdot x\text{C}_6\text{H}_5\text{NO}_2$ , *J. Am. Chem. Soc.*, 1990, **112**, 1546–1554.

79 B. Hribar, N. T. Southall, V. Vlachy and K. A. Dill, How ions affect the structure of water, *J. Am. Chem. Soc.*, 2002, **124**, 12302–12311.

80 R. Custelcean and B. A. Moyer, Anion separation with metal–organic frameworks, *Eur. J. Inorg. Chem.*, 2007, 1321–1340.

81 T. Kotabe, Y. Ogasawara, K. Suzuki, S. Uchida, N. Mizuno and K. Yamaguchi, Porous cubic cesium salts of silicododecatungstate(molybdate)/borododecatungstate blends: Synthesis and molecular adsorption properties, *Inorg. Chem.*, 2018, **57**, 8821–8830.

